Journal of Applied Physics

RESEARCH ARTICLE | AUGUST 24 2015

Epitaxial growth of phase-pure ε-Ga_2O_3 by halide vapor phase epitaxy

Yuichi Oshima; Encarnación G. Víllora; Yoshitaka Matsushita; Satoshi Yamamoto; Kiyoshi Shimamura

J. Appl. Phys. 118, 085301 (2015)
https://doi.org/10.1063/1.4929417

Epitaxial growth of phase-pure ε-Ga_2O_3 by halide vapor phase epitaxy

Yuichi Oshima,[1,a)] Encarnación G. Víllora,[1] Yoshitaka Matsushita,[2] Satoshi Yamamoto,[3] and Kiyoshi Shimamura[1]
[1]*Optical Single Crystals Group, National Institute for Materials Science, 1-1 Namiki, Tsukuba, Ibaraki 305-0044, Japan*
[2]*Materials Analysis Station, National Institute for Materials Science, 1-1 Namiki, Tsukuba, Ibaraki 305-0044, Japan*
[3]*Optoelectronic Materials Group, National Institute for Materials Science, 1-1 Namiki, Tsukuba, Ibaraki 305-0044, Japan*

(Received 18 July 2015; accepted 11 August 2015; published online 24 August 2015)

Epitaxial growth of ε-Ga_2O_3 is demonstrated for the first time. The ε-Ga_2O_3 films are grown on GaN (0001), AlN (0001), and β-Ga_2O_3 ($\bar{2}01$) by halide vapor phase epitaxy at 550 °C using gallium chloride and O_2 as precursors. X-ray ω-2θ and pole figure measurements prove that phase-pure ε-Ga_2O_3 (0001) films are epitaxially grown on the three kinds of substrates, although some minor misoriented domains are observed. High temperature X-ray diffraction measurements reveal that the ε-Ga_2O_3 is thermally stable up to approximately 700 °C. The optical bandgap of ε-Ga_2O_3 is determined for the first time to be 4.9 eV. © *2015 AIP Publishing LLC*.
[http://dx.doi.org/10.1063/1.4929417]

I. INTRODUCTION

Ga_2O_3 has been reported to possess five different crystal structures, namely, α-, β-, δ-, ε-, and γ-phase.[1] Among them, β-Ga_2O_3 crystallizes in the monoclinic structure (space group $C2/m$) and is believed to be thermodynamically the most stable under atmospheric pressure. β-Ga_2O_3 has a bandgap energy as large as 4.7–4.9 eV, and therefore, it exhibits a wide transparency even in the UV region.[2–4] In addition, β-Ga_2O_3 is a semiconductor, with Si and Sn as the most efficient donors.[5,6] Furthermore, high-quality single crystalline wafers can be produced through melt growth techniques.[7–9] These unique features make this material a suitable and promising wide bandgap semiconductor for diverse applications such as conductive transparent substrates for GaN-based high-performance LEDs,[10,11] and solar-blind UV sensors.[12] Above and beyond these, β-Ga_2O_3 is also attracting a remarkable attention due to its great potential to realize power devices with higher breakdown voltages and lower energy losses than its counterparts GaN and SiC.[13–15]

In contrast to β-Ga_2O_3, there are only a limited number of reports on ε-Ga_2O_3, the target material of this work. ε-Ga_2O_3 is one of the meta-stable phases of Ga_2O_3, which was first synthesized by Roy *et al*. through the thermal decomposition of $Ga(NO_3)_3$.[1] Although they indicated a high thermal stability of their ε-Ga_2O_3 up to 870 °C, the full structural characterization was not made, and the crystal structure remained unclear for over half a century. Recently, Playford *et al*. carried out the structural analysis of their powder material synthesized through the thermal decomposition of $Ga(NO_3)_3{\cdot}9H_2O$, and finally identified the crystal structure of ε-Ga_2O_3, belonging to the high symmetry hexagonal system with space group $P6_3mc$ (PDF# 01–082-3196),[16] like hexagonal GaN. In any case, the samples prepared by both authors suffered from low phase-purity. Even the best material of Playford *et al*. was still a mixture of ε-Ga_2O_3 (57%) and β-Ga_2O_3 (43%).

As described above, the synthesis of ε-Ga_2O_3 has so far been limited to powdered materials with a lack of phase-purity, so that, till date, even very fundamental properties, such as the bandgap energy, are still unknown. However, the ε-phase is expected to have a sufficient thermal stability for practical device applications, and therefore, ε-Ga_2O_3 could be a wide bandgap semiconductor as promising as β-Ga_2O_3. In order to clarify the material properties, first of all, a synthesis technique which enables the effective growth of ε-Ga_2O_3 with high phase-purity and low impurity concentrations has to be established. On top of that, it is necessary to develop an epitaxial growth technique to deposit this material for semiconductor device applications.

In this work, we employed halide vapor phase epitaxy (HVPE) as the growth method of ε-Ga_2O_3. HVPE is a type of chemical vapor deposition (CVD), which has been widely used to grow high-quality epilayers with large growth rates in the III-V compound semiconductor industry.[17,18] Recently, HVPE has been successfully applied for the growth of β-Ga_2O_3[19–21] and even α-Ga_2O_3.[22] The present work is the first report on the epitaxial growth of ε-Ga_2O_3 layers.

II. EXPERIMENTAL METHOD

The HVPE growth was carried out in a horizontal atmospheric reactor at 550 °C using gallium chloride and O_2 (>99.99995% pure) as precursors. The gallium chloride was synthesized *in situ* upstream in the reactor through the chemical reaction between Ga (>99.99999% pure) and HCl (>99.999% pure). The HCl and O_2 were supplied with partial pressures of 0.25 kPa and 1.0 kPa, respectively. N_2 (>99.9999% pure) was flown together with the precursors as

a)Electronic mail: OSHIMA.Yuichi@nims.go.jp

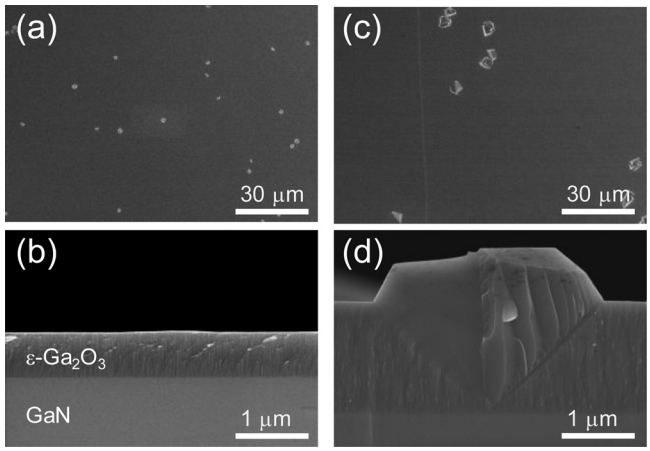

FIG. 1. SEM images of ε-Ga_2O_3 layers grown on GaN (0001) with different growth times: (a) and (b) 2 min; and (c) and (d) 7 min.

the carrier gas. The growth times were 2 min or 7 min. Three different substrates were tried, namely, *c*-plane GaN substrates, *c*-plane AlN(13-μm-thick)/SiC templates, and ($\bar{2}$01) β-Ga_2O_3 substrates.

The surface and the cross-section of the films were observed by scanning electron microscopy (SEM). The crystal structure and the orientation were investigated by X-ray diffraction (XRD) ω-2θ scan and pole-figure measurements. The structural quality was estimated by X-ray rocking curve (XRC) measurements. To clarify the thermal stability of the ε-Ga_2O_3, high-temperature X-ray diffraction (HT-XRD) studies were carried out. The sample was set on a Pt holder and its temperature was elevated from room temperature up to 1300 °C stepwise, with 30 min intervals for temperature stabilization. The XRD patterns were recorded under air in the standard ω-2θ scan mode. Impurity concentrations were evaluated by secondary mass spectrometry (SIMS). The optical bandgap was determined by means of a transmittance measurement.

III. RESULTS AND DISCUSSION

SEM images of the surface and the cross-section of the films grown on GaN (0001) for 2 min and 7 min are shown in Figs. 1(a)–1(d), respectively. Smooth compact layers were successfully grown, although some three-dimensional (3D) grains can be observed on the surface. The growth rate of the film was estimated to be approximately 20 μm/h from Fig. 1(d). The crystal structure and the orientation of the 3D-grains are unclear at present. As can be seen in Fig. 1(d), these are originated at the interface with the substrate; thus,

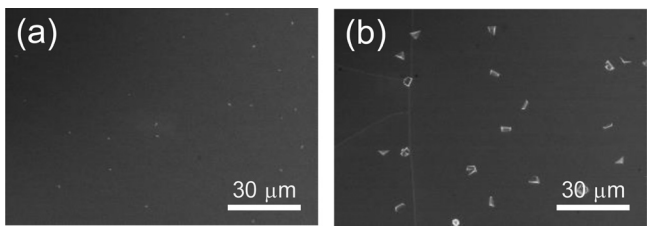

FIG. 2. SEM images of ε-Ga_2O_3 layers grown on AlN (0001) with different growth times: (a) 2 min and (b) 7 min.

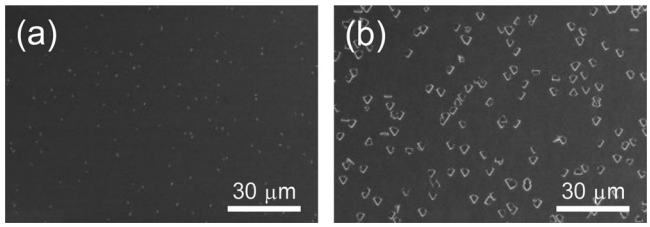

FIG. 3. SEM images of ε-Ga_2O_3 layers grown on β-Ga_2O_3 ($\bar{2}$01) with different growth times: (a) 2 min and (b) 7 min.

their surface density was independent of the growth time. Furthermore, as the 3D-grains grew laterally and vertically faster than the epilayer, the grain-size increased continuously, becoming more protruding with the growth time. Therefore, it is necessary to improve the growth conditions at the early growth stage, during the nucleation, in order to suppress the formation of the 3D-grains.

Figures 2 and 3 show top-view SEM images of the films deposited on AlN (0001) and β-Ga_2O_3 ($\bar{2}$01), respectively. The morphologies were similar to that of the film grown on GaN (0001); however, the 3D-grain density on β-Ga_2O_3 ($\bar{2}$01) was significantly higher. In the following, only the results on the 7-min-grown samples (approximately 2.3 μm thick) are described, unless otherwise specified.

Figure 4 shows the XRD ω-2θ scan profiles of the HVPE-grown films on the three kinds of substrates. In all of these cases, apart from the diffraction peaks corresponding to the substrates, only the diffraction peaks from ε-Ga_2O_3 (0001) appeared, and no other polymorphs of Ga_2O_3 were detected.

The pole figures of the ε-Ga_2O_3 film and the corresponding GaN substrate are shown in Figs. 5(a) and 5(b), respectively. Diffraction spots of ε-Ga_2O_3 *10$\bar{1}$4* appeared only at the positions expected for single crystalline ε-Ga_2O_3. The 3D-grains observed by SEM in Figs. 1(a) and 1(c) may be misoriented domains of ε-Ga_2O_3, but no corresponding peaks were detected probably due to the small volume fraction.

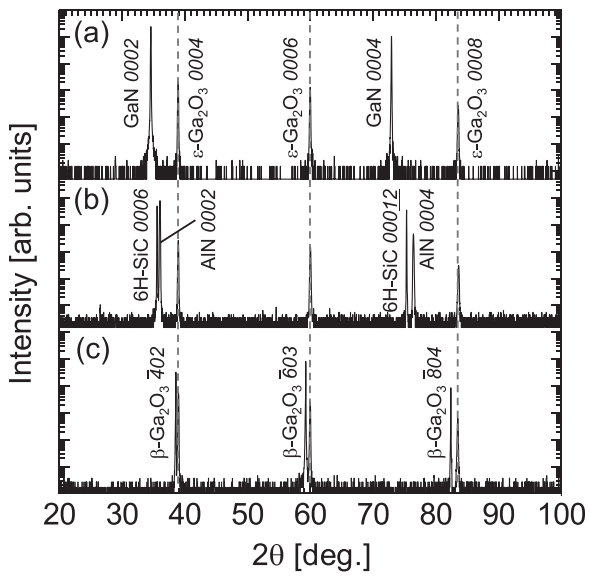

FIG. 4. XRD ω-2θ scan profiles of ε-Ga_2O_3 layers grown on (a) GaN (0001), (b) AlN (0001), and (c) β-Ga_2O_3 ($\bar{2}$01).

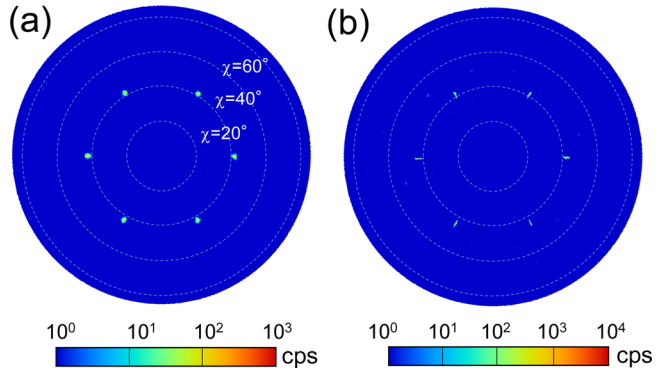

FIG. 5. X-ray pole figures (log-scale) of (a) ε-Ga_2O_3 $10\bar{1}4$ and (b) GaN $10\bar{1}2$.

The comparison of the peak positions in Figs. 5(a) and 5(b) revealed the following epitaxial relationships: ε-Ga_2O_3 (0001)||GaN (0001) and ε-Ga_2O_3 [$10\bar{1}0$]||GaN [$10\bar{1}0$]. Analogously, the pole figures of the ε-Ga_2O_3 film and the corresponding AlN (0001) template were similar (Figs. 6(a) and 6(b)), and the epitaxial relationships were elucidated to be equally ε-Ga_2O_3 (0001)||AlN (0001) and ε-Ga_2O_3 [$10\bar{1}0$]||AlN [$10\bar{1}0$]. The in-plane lattice mismatches are 8.8 and 6.6% with GaN (0001) and AlN(0001), respectively.

Figures 7(a) and 7(b) show the pole figures of the ε-Ga_2O_3 film and the corresponding β-Ga_2O_3 ($\bar{2}01$) substrate, respectively. In contrast with the case on the GaN and AlN substrates, additional very small diffraction peaks of ε-Ga_2O_3 were detected probably due to the larger volume fraction of the 3D-grains. The epitaxial relationships between the c-plane ε-Ga_2O_3 and the substrate were determined to be ε-Ga_2O_3 (0001)||β-Ga_2O_3 ($\bar{2}01$) and ε-Ga_2O_3 [$10\bar{1}0$]||β-Ga_2O_3 [102]. This result is in good accordance with the observed growth of hexagonal GaN on the same substrate.[23] Further, the in-plane atomic arrangement of Ga or O in both ε-Ga_2O_3 (0001) and β-Ga_2O_3 ($\bar{2}01$) are virtually triangular lattices, and the mismatch is as small as 1.1%.

It is worth mentioning that the crystal structure of Ga_2O_3 has been reported to suit that of the substrate flexibly. For example, corundum-structured α-Ga_2O_3 was grown on c-plane sapphire under the same growth conditions as in the present work.[22] It is also reported that cubic γ-Ga_2O_3 was grown on spinel (100) (the both materials belong to the same

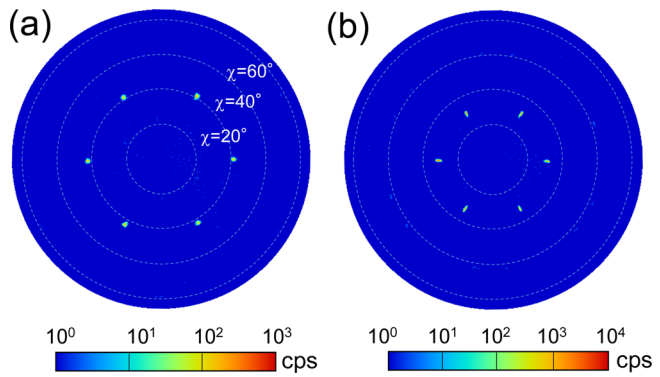

FIG. 6. X-ray pole figures (log-scale) of (a) ε-Ga_2O_3 $10\bar{1}4$ and (b) AlN $10\bar{1}3$.

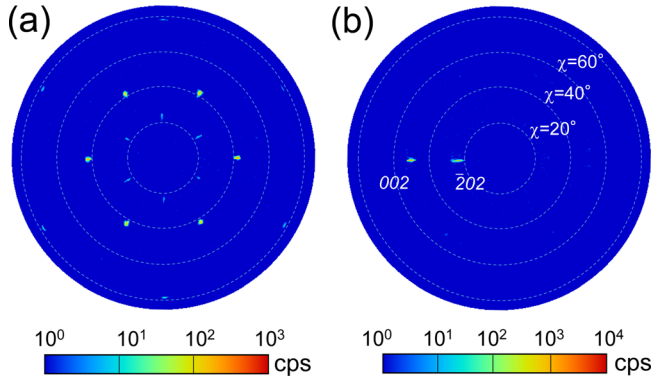

FIG. 7. X-ray pole figures (log-scale) of (a) ε-Ga_2O_3 $10\bar{1}4$ and (b) β-Ga_2O_3 002. Note that the β-Ga_2O_3 $\bar{2}02$ peak also appears because the (001) and ($\bar{1}$01) planes have almost the same spacing and thus the same Bragg angle.

space group $Fd\bar{3}m$) by mist-CVD, while α-Ga_2O_3 was grown on c-plane sapphire under the similar growth condition.[24] Therefore, it seems natural that ε-Ga_2O_3 can grow on GaN and AlN, since all belong to the same space group $P6_3mc$. However, at first sight, it is surprising that ε-Ga_2O_3 grows "heteroepitaxially" on β-Ga_2O_3, which is believed to be the most stable polymorph of Ga_2O_3. It should be noted that the use of similar growth conditions, except for the higher growth temperatures around 1050 °C, leads to the growth of the β-phase.[21] Further investigations including the surface structure of β-Ga_2O_3 ($\bar{2}01$) at the atomic level in the growth atmosphere of HVPE will be needed to clarify the mechanism of this unusual phenomenon.

The XRC profiles of the ε-Ga_2O_3 0004 and $10\bar{1}1$ diffractions, which were measured in symmetric and skew-symmetric geometries, respectively, are shown in Fig. 8. The FWHMs of 0004 and $10\bar{1}1$ diffractions reflect the tilting of c-plane and the twisting around the c-axis, respectively. The FWHMs of ε-Ga_2O_3 grown on GaN and AlN were similar,

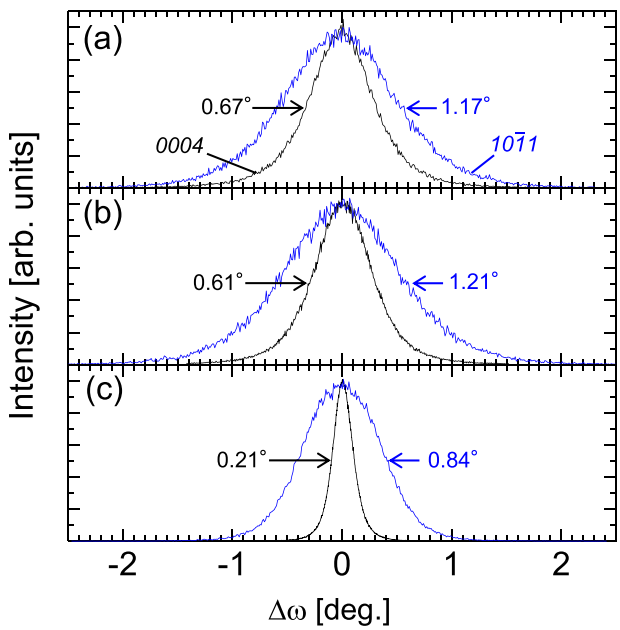

FIG. 8. XRCs of ε-Ga_2O_3 layers grown on (a) GaN (0001), (b) AlN (0001), and (c) β-Ga_2O_3 ($\bar{2}01$).

while those of ε-Ga_2O_3 deposited on β-Ga_2O_3 were much smaller. This tendency agrees well with that of the in-plane lattice mismatch. Note that the *0004* XRC profile of the ε-Ga_2O_3 grown on β-Ga_2O_3 ($\bar{2}01$) was measured around the rocking axis of β-Ga_2O_3 [010], and the FWHM was not significantly different from that measured around the perpendicular rocking axis of β-Ga_2O_3 [102].

Figure 9 shows the result of the HT-XRD measurements of the ε-Ga_2O_3 grown on GaN. Apart from the substrate and Pt holder diffractions, the spectra are dominated by the diffraction peak of ε-Ga_2O_3 up to 700 °C. With the further increase of temperature, the β-Ga_2O_3 *401* peak appears and its intensity increases with the temperature up to around 800 °C. Inversely, the intensity of the ε-Ga_2O_3 *0004* diffraction peak starts to decrease above 700 °C, and virtually disappears around 800 °C. Thus, the HVPE-grown ε-Ga_2O_3 is found to be thermally stable up to around 700 °C, and it transforms into β-Ga_2O_3 at higher temperatures. The reported transition temperature from ε-Ga_2O_3 to β-Ga_2O_3 varies depending on the authors. Roy *et al*. and Playford *et al*. reported the temperature to be 870 °C (Ref. 1) and above 500 °C,[16] respectively. Their samples were synthesized by the thermal decomposition of gallium nitrate, and therefore, the impurities and their concentrations are probably different from those in HVPE-grown ε-Ga_2O_3. Such difference could be the origin of the different transition temperatures, since impurities sometimes affect the crystal structure of Ga_2O_3. For example, Hayashi *et al*. demonstrated the growth of Mn-doped γ-Ga_2O_3 (7 at. %) on *c*-plane sapphire by pulsed laser deposition, while their un-doped sample crystalized in the β-Ga_2O_3 phase.[25]

Table I summarizes the impurity concentrations in ε-Ga_2O_3 grown on GaN measured by SIMS. [C], [N], [Si], [Al], [Cr], [Fe], and [Ni] were below the detection limits. [H] and [Cl] were relatively higher than those in α-Ga_2O_3 grown under the same growth conditions in the same HVPE reactor ($[H] < 4 \times 10^{17}$, $[Cl] = 7 \times 10^{16}$).[22] Although the influence of H or Cl impurities on the electrical properties of ε-Ga_2O_3 has not clarified yet, it is worth mentioning that Murakami *et al*. has also reported the incorporation of Cl impurity in HVPE-grown β-Ga_2O_3, and that this did not act as a donor.[20]

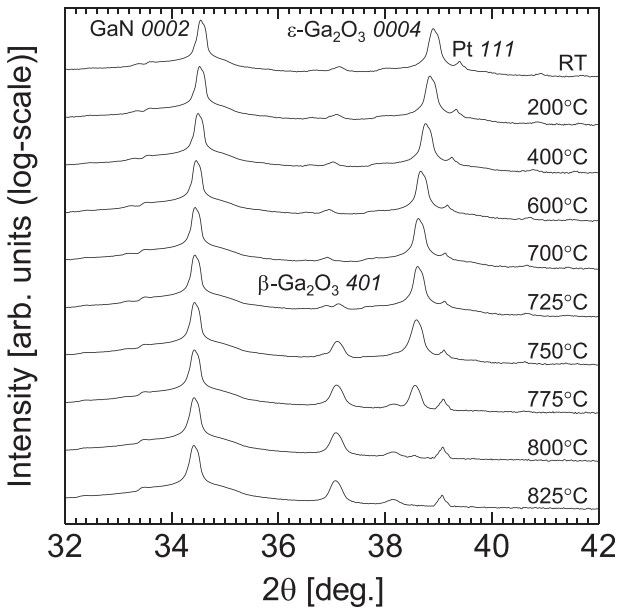

FIG. 9. HT-XRD of ε-Ga_2O_3 grown on GaN (0001).

TABLE I. Impurity concentrations in ε-Ga_2O_3 measured by SIMS.

Element	Possible origin	Detection limit (D. L.) (cm^{-3})	Concentration (cm^{-3})
H	HCl	4×10^{17}	1×10^{18}
C	SiC, graphite	6×10^{16}	<D. L.
N	GaN, AlN	5×10^{16}	<D. L.
Al	AlN	3×10^{15}	<D. L.
Si	Quartz	1×10^{16}	<D. L.
Cl	HCl	1×10^{16}	2×10^{18}
Cr	Stainless steel	4×10^{14}	<D. L.
Fe	Stainless steel	8×10^{14}	<D. L.
Ni	Stainless steel	3×10^{15}	<D. L.

The transmittance spectrum of ε-Ga_2O_3 grown on AlN(0001)/SiC template for 2 min is shown in Fig. 10. Prior to the measurement, the SiC substrate was removed by lapping and polishing in order to avoid the absorption cutoff of this. Although the transition type of ε-Ga_2O_3 is still unknown, we estimated the bandgap energy to be 4.9 eV from the $(h\nu\alpha)^2$–$h\nu$ plot (inset of Fig. 10), in which the liner fitting is much better than that in $(h\nu\alpha)^{1/2}$–$h\nu$ plot (not shown). This result indicates that the bandgap energy is similar to that of β-Ga_2O_3, and therefore, opto-electrical properties in general might be comparable for both phases.

IV. SUMMARY

In conclusion, the present investigation demonstrates for the first time the successful epitaxial growth of phase-pure ε-Ga_2O_3. The epilayers were deposited by the HVPE method, achieving a growth rate as high as 20 μm/h. It was found that the use of *c*-plane GaN and AlN substrates, whose space group is the same as that of ε-Ga_2O_3, is one of the key points to deposit ε-Ga_2O_3 epitaxial layers. The second critical parameter was the deposition temperature, so that ε-Ga_2O_3 could be grown heteroepitaxially even on β-Ga_2O_3 ($\bar{2}01$) substrates. It

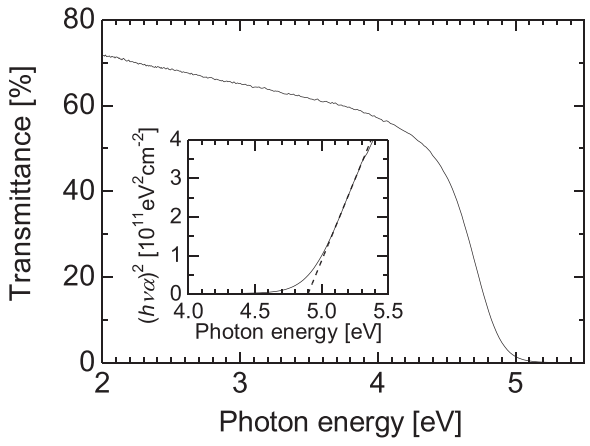

FIG. 10. Transmittance spectra of ε-Ga_2O_3. The inset shows the absorption coefficient in $(h\nu\alpha)^2$ vs $h\nu$.

was found that the ε-Ga_2O_3 film grown on β-Ga_2O_3 ($\bar{2}01$) exhibits better XRC-FWHM compared to those of the ε-Ga_2O_3 films grown on GaN and AlN, probably due to the smaller lattice mismatch, although the volume fraction of the 3D-grains, which are considered to be misoriented domains, was significantly higher than that on other two substrates. HT-XRD measurement revealed the high thermal stability of the ε-Ga_2O_3 films up to around 700 °C. The result of SIMS measurement showed that [H] and [Cl] were relatively higher than those in α-Ga_2O_3 grown under the same growth conditions, while [C], [N], [Si], [Al], [Cr], [Fe], and [Ni] were below the detection limits. The optical bandgap was determined for the first time to be 4.9 eV, which is comparable to that of β-Ga_2O_3. These results prove the superior effectiveness of HVPE as epitaxial growth technique for ε-Ga_2O_3, and further suggest that ε-Ga_2O_3 can be a new promising wide bandgap semiconductor.

ACKNOWLEDGMENTS

This work was partly supported by a Grant-in-Aid for Scientific Research (C) No. 25420307 from Japan Society for the Promotion of Science (JSPS).

[1]R. Roy, V. G. Hill, and E. F. Osborn, J. Am. Chem. Soc. **74**, 719 (1952).
[2]H. H. Tippins, Phys. Rev. **140**, A316 (1965).
[3]M. R. Lorenz, J. F. Woods, and R. J. Gambino, J. Phys. Chem. Solids **28**, 403 (1967).
[4]M. Orita, H. Ohta, M. Hirano, and H. Hosono, Appl. Phys. Lett. **77**, 4166 (2000).
[5]N. Suzuki, S. Ohira, M. Tanaka, T. Sugawara, K. Nakajima, and T. Shishido, Phys. Status Solidi C **4**, 2310 (2007).
[6]E. G. Víllora, K. Shimamura, Y. Yoshikawa, T. Ujiie, and K. Aoki, Appl. Phys. Lett. **92**, 202120 (2008).
[7]H. Aida, K. Nishiguchi, H. Takeda, N. Aota, K. Sunakawa, and Y. Yaguchi, Jpn. J. Appl. Phys., Part 1 **47**, 8506 (2008).
[8]E. G. Víllora, K. Shimamura, Y. Yoshikawa, K. Aoki, and N. Ichinose, J. Cryst. Growth **270**, 420 (2004).
[9]Z. Galazka, K. Irmscher, R. Uecker, R. Bertram, M. Pietsch, A. Kwasniewski, M. Naumann, T. Schulz, R. Schewski, D. Klimm, and M. Bickermann, J. Cryst. Growth **404**, 184 (2014).
[10]K. Shimamura, E. G. Víllora, K. Domen, K. Yui, K. Aoki, and N. Ichinose, Jpn. J. Appl. Phys., Part 2 **44**, L7 (2005).
[11]E. G. Víllora, S. Arjoca, K. Shimamura, D. Inomata, and K. Aoki, Proc. SPIE **8987**, 89871U (2014).
[12]T. Oshima, T. Okuno, N. Arai, N. Suzuki, S. Ohira, and S. Fujita, Appl. Phys. Express **1**, 011202 (2008).
[13]K. Sasaki, A. Kuramata, T. Masui, E. G. Víllora, K. Shimamura, and S. Yamakoshi, Appl. Phys. Express **5**, 035502 (2012).
[14]M. Higashiwaki, K. Sasaki, A. Kuramata, T. Masui, and S. Yamakoshi, Appl. Phys. Lett. **100**, 013504 (2012).
[15]M. Higashiwaki, K. Sasaki, T. Kamimura, M. H. Wong, D. Krishnamurthy, A. Kuramata, T. Masui, and S. Yamakoshi, Appl. Phys. Lett. **103**, 123511 (2013).
[16]H. Y. Playford, A. C. Hannon, E. R. Barney, and R. I. Walton, Chem. Eur. J. **19**, 2803 (2013).
[17]Y. Oshima, T. Eri, M. Shibata, H. Sunakawa, K. Kobayashi, T. Ichihashi, and A. Usui, Jpn. J. Appl. Phys., Part 2 **42**, L1 (2003).
[18]K. Motoki, T. Okahisa, R. Hirota, S. Nakahata, K. Uematsu, and N. Matsumoto, J. Cryst. Growth **305**, 377 (2007).
[19]K. Nomura, K. Goto, R. Togashi, H. Murakami, Y. Kumagai, A. Kuramata, S. Yamakoshi, and A. Koukitu, J. Cryst. Growth **405**, 19 (2014).
[20]H. Murakami, K. Nomura, K. Goto, K. Sasaki, K. Kawara, Q. T. Thieu, R. Togashi, Y. Kumagai, M. Higashiwaki, A. Kuramata, S. Yamakoshi, B. Monemar, and A. Koukitu, Appl. Phys. Express **8**, 015503 (2015).
[21]Y. Oshima., E. G. Víllora, and K. Shimamura, J. Cryst. Growth **410**, 53 (2015).
[22]Y. Oshima., E. G. Víllora, and K. Shimamura, Appl. Phys. Express **8**, 055501 (2015).
[23]M. M. Muhammed, M. Peres, Y. Yamashita, Y. Morishima, S. Sato, N. Franco, K. Lorenz, A. Kuramata, and I. S. Roqan, Appl. Phys. Lett. **105**, 042112 (2014).
[24]T. Oshima, T. Nakazono, A. Mukai, and A. Ohtomo, J. Cryst. Growth **359**, 60 (2012).
[25]H. Hayashi, R. Huang, H. Ikeno, F. Oba, S. Yoshioka, I. o Tanaka, and S. Sonoda, Appl. Phys. Lett. **89**, 181903 (2006).